Comparison of GRACE Derived Greenland Mass Wasting to Physical Drivers of Ice Loss From MERRA-2 Reanalysis

Benjamin Getraer

Senior Thesis Draft

Presented to the Faculty

of Princeton University

in Candidacy for the Degree

of Bachelor of Arts

Recommended for Acceptance

by the Department of

Geosciences

Adviser: Laure Resplandy

Second Reader: Frederik J. Simons

April 16, 2019

This paper represents my own work in accordance with University regulations,

Benjamin Getraer

Abstract

Melting ice from the Greenland Ice-Sheet has accounted for an increasing percentage — now estimated at 25% — of rising global mean sea-level since the early 1990s. As recently as 2016, gravimetric and altimetric studies of Greenland melting rates found increasing rates of ice loss, which have not been borne out in GRACE gravimetric observations over the last few years (2015–2017). We hypothesize that the true trend of Greenland ice loss between 2003–2017 is linear, and that deviations from the linear trend may be explained by inter-annual variability in climate. We demonstrate a novel application of 2-dimensional discrete wavelet analysis to the GRACE dataset to recover spatial structure of inter-annual variability in ice loss, focusing on the unusual melt and accumulation seasons of 2012–2014. Finally, we compare our interpretation of the 2012–2014 anomaly in spatial scale and location to the results of others using independent atmospheric, altimetric, and meteorologic data sources.

Key Points:

1. We focus on inter-annual variability of the Greenland ice loss trend.
2. We analyze subregional signals using discrete wavelet transforms.
3. We define the 2012–2014 anomaly in spatial structure.

Acknowledgements

Contents

List of Figures

List of Tables

Introduction

Data

Ice Mass Data

Observations of ice loss across large areas are measured remotely by satellites using several different methods, including weighing the mass by gravitational anomaly (such as NASA's GRACE and GRACE Follow-On missions), photographing surface area (such as NASA's Landsat and MODIS missions), and by measuring relative height of the ice with active laser altimetry (such as NASA's ICESat and ICESat-2 missions) (Khan et al., 2015).

Atmospheric Data

In addition to datasets which directly measure physical manifestations of ice sheet melting, there are complimentary datasets which capture some of the processes which control melting such as air temperature, humidity, and cloud cover. The primary atmospheric data used in this study are reanalysis products from the Modern-Era Retrospective analysis for Research and Applications, Version 2 (MERRA-2) (see Table 1 and Appendix A: Data and code sources).

Variable	**Temporal Resolution**	**Dataset**
2 Meter Air Temperature	daily	tavg1_2d_slv_Nx
	monthly	statM_2d_slv_Nx
500 hPa Air Temperature	daily	tavg1_2d_slv_Nx
2 Meter Air Specific Humidity	daily	tavg1_2d_slv_Nx
500 hPa Air Specific Humidity	daily	tavg1_2d_slv_Nx
Skin Surface Temperature	daily	tavg1_2d_slv_Nx
Total Cloud Area Fraction	daily	tavg1_2d_rad_Nx
Surface Net Downward Shortwave Flux	daily	tavg1_2d_rad_Nx

Table 1: MERRA-2 data used in this study (see Appendix A: Data and code sources). Mean daily and monthly values were accessed on the default MERRA-2 $0.625°$ lon$\times$$0.5°$ lat grid with an original spatial resolution of approximately 50 km$\times$50 km(Bosilovich et al., 2016). Values are based on the GEOS climate models which combine direct observations into a globally continuous representation of the atmosphere, ocean, and surface interactions using a consistent set of of conservation assumptions (Bosilovich et al., 2016; Gelaro et al., 2017).

“Reanalysis” refers to a way of processing an ensemble of directly measured weather observations using a consistent set of rules that assume physical constraints on the ways in which different atmospheric variables interact temporally and spatially (Gelaro et al., 2017). These physical constraints are defined by a global climate model, which can both make forecasts of future developments of meteorological variables and output modeled solutions based on weather measurements directly observed at weather stations all over the world (Gelaro et al., 2017). Variable values for a given time and spatial location are calculated as a best fit of direct observations to the constraints of multiple different models which define processes such as radiation balances, physical movement, chemical interactions, precipitation, and so forth, or are inferred by the models’ rules from variables which are directly measured (Bosilovich et al., 2016; Gelaro et al., 2017).

The data for this study come from NASA’s Global Modeling and Assimilation Office’s Goddard Earth Observing System (GEOS) climate models, and are publicly available in specific MERRA-2 data products through the NASA Goddard Earth Sciences Data Information Services Center (GES DISC) (see Appendix A: Data and code sources). MERRA-2 data are available in several different spatial and temporal formats for different variables. I use gridded daily averages for examining the connections between meteorological variables over the Greenland Ice Sheet, and gridded monthly averages for capturing the long-term development of Greenland’s climate. Daily and monthly data are taken from collections of single-level, two-dimensional data which GES DISC provides in a few MERRA-2 datasets (see Table 1, Appendix A: Data and code sources).

Daily and monthly NAO climate index values are provided by the National Weather Service Climate Prediction Center, which calculates NAO index values from the 500 mb pressure level height over the spatial extent of 20–90° N (CPC, 2012). Pressure level heights are compared to a monthly loading pattern defined as the first principal component of a rotated principal component analysis on the 1950–2000 500 mb height time-series and values are normalized by monthly mean and standard of deviation for the 1950–2000 index time-series (see Appendix A: Data and code sources and CPC, 2012).

Lastly, Northern Hemisphere climate data are from the Goddard Institute for Space Studies Surface Temperature Analysis (GISTEMP v3) as a mean monthly Land-Ocean Temperature Index (LOTI), which takes into account dampening of atmospheric temperature changes due to the heat capacity of ocean water (Hansen et al., 2010). The data used here are a monthly index of temperature anomalies from 1951–1980 time-series, which are available from 1880–present (see Appendix A: Data and code sources and Hansen et al., 2010).

Methods

All analysis of MERRA-2 data over the Greenland Ice Sheet was masked using a widely-used shape-file of the ice sheet developed from the drainage subregions defined by Zwally et al. (2012), reorganized into quadrants similar to McMillan et al. (2016) (see Figure 1).

Results

Near Surface Temperature Trends Since 1980

Over the 1980–2017 time period the Northern Hemisphere has been gradually warming, and averaging across the monthly LOTI anomaly with 10 year moving window reveals a quite linear trend of 0.24°C per decade (type 1 least-squares regression, with a variance reduction $R^2 = 0.987$), for a total increase of 0.89°C since 1980 (see Figure 2). Over the same time period, near surface temperature anomalies over the Greenland Ice Sheet had a significantly different pattern of increase, remaining static through the 1980's and more recently since the early 2000's, and increasing dramatically through the 1990's (Figure 2). Comparing the first 15 years (1980–1994) of the 1980–2017 time period to the last 15 years (2003–2017), the mean temperature rose 1.53 ± 0.42°C as illustrated in Figure 2 (two sample t-test found distributions of significantly

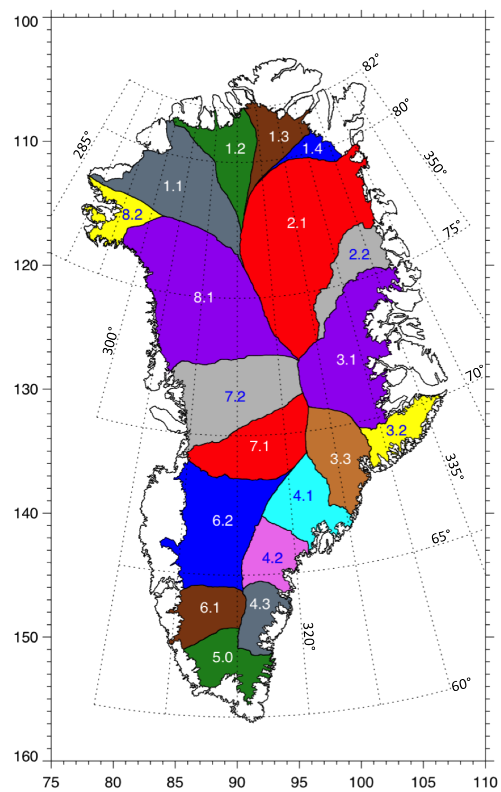

Figure 1: Drainage subregions of Greenland used to define ice sheet extent and quadrants in this paper (figure and data from Zwally et al., 2012). Quadrants used in this paper are unions of these subregions as follows: NW $= \cup(1.1, 1.2)$; NE $= \cup(1.3, 1.4, 2.1, 2.2)$; SE $= \cup(3.1, 3.2, 3.3, 4.1, 4.2, 4.3)$; SW $= \cup(5.0, 6.1, 6.2, 7.1, 7.2)$, similar to the divisions made in McMillan et al. (2016).

different mean values, $p = 2.3\text{e}{-12}$; reported error represents the 95% confidence interval on the difference in mean values).

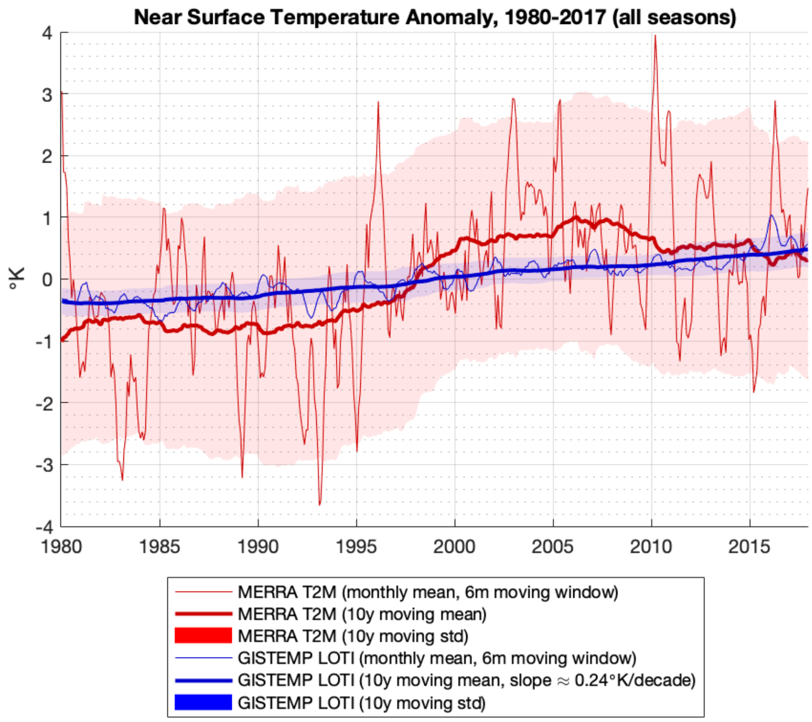

Figure 2: Mean monthly near surface temperature anomalies for the Northern Hemisphere (GISTEMP Land-Ocean Temperare Index, blue) and the Greenland Ice Sheet (MERRA-2 2m air temperature, red), 1980–2017. Data has been filtered using 6-month and 10-year moving windows for ease of interpretation, with the shaded area representing the spread of the data using the standard of deviation of the 10-year moving window. Note the more continuously linear increase in Northern Hemisphere temperature over the entire time-period compared to the non-linear jump in temperature over Greenland in the 1990's. Analyses of the unfiltered time-series show that: the Northern Hemisphere LOTI is increasing at 0.24°C per decade ($R^2 = 0.987$); near-surface air temperature increased 1.53 ± 0.42°C between the years 1980–1994 and 2003–2017.

Rise in near surface air temperature across the Greenland Ice Sheet between 1980–2017 differed seasonally, with the greatest rise in temperature occurring in the Winter season (December, January, February) and the smallest rise in temperature occuring in the Summer season (June, July, August) (see Figure 3). The fitted linear trends were tested for significance against the hypothesis that a trend of the same magnitude could be generated from similar random data (normally distributed data of the same mean, standard of deviation, and number of points). p-values for the trends represent the percentage of trends of greater magnitude found in 10000 tests of similar random data (the trend slope of greatest absolute value would have $p(\max) = 0$, and a trend slope of 0 would have $p(0) = 1$). A similar method was used to calculate the confidence interval of these trends, by subtracting the linear fit, generating 10000 tests of similar random data, and finding the 90^{th} and 95^{th} percentile of slope magnitude amongst the random test data.

For the seasonal near surface air temperature trends between 1980–2017, all were found to be significant at at least the $p < 0.05$ threshold compared to the 10000 tests of similar random data (see Table 2). The difference in trend between Winter and Summer months is significant in the random simulations, with the best fit trend for each falling outside of the 90% confidence interval of the other (see Table 2).

Season	**Trend [°C/decade]**	95% **conf. int.**	90% **conf. int.**	p**-value**
		1980–2017		
Winter (DJF)	+0.80	±0.46	±0.38	0.0015
Spring (MAM)	+0.46	±0.36	±0.30	0.0163
Summer (JJA)	+0.35	±0.17	±0.15	0.0002
Fall (SON)	+0.48	±0.29	±0.25	0.0021
		2003–2017		
Winter (DJF)	−0.60	±1.12	±0.93	0.413
Spring (MAM)	−0.98	±1.11	±0.94	0.105
Summer (JJA)	−0.72	±1.13	±0.94	0.217
Fall (SON)	−0.02	±1.13	±0.94	0.971

Table 2: Seasonal trends in MERRA-2 2m air temperature calculated on mean monthly data across the Greenland Ice Sheet for the time period 1980–2017 and 2003–2017, shown in Figure 3. The trend is the type 1 least squares regression slope of the mean monthly data, and confidence intervals are the results of synthetic data tests analyzing the residuals of the data and the trend line. p-values represent the chances of finding a trend slope of equal or greater magnitude in a random sampling of a "similar" normal distribution. For 1980–2017, all seasons have trend magnitudes that are significantly different from a random sampling of a "similar" normal distribution at the $p < 0.05$ threshold; Winter and Summer seasonal trends are significantly different from each other at the 90% confidence interval; Fall and Spring trends are not significantly different from Summer, and are not well differentiated from Winter. For 2003–2017, Winter and Fall trends are well within expected fits for similar random data, and while the Spring and Summer trends are more unusual, those negative trends are also not significantly differentiable from similar random data in p-value or confidence interval.

Despite the overall rise in temperature since the 1980's, near surface air temperature across the Greenland Ice Sheet was not increasing over the GRACE record (2003–2017) (Figure 3). In fact, mean 2m air temperature anomaly over the ice sheet drifted cooler in every season, most markedly in Spring and Summer (see Figure 3 & Table 2). The cooling drift in temperature from 2003–2017 was analyzed for significance in the same manner as the trends over the entire

1980–2017 record (Table 2). The trends in Winter and Fall were indistinguishable from similar random data drawn from a normal distribution of the same mean and standard of deviation, and while the trends in Spring and Summer were more unusual for random variability, they too were poorly differentiated from similar random data in both p-value and confidence interval (Table 2).

Taking into consideration the probability of random simultaneous negative drift in 2m air temperature anomaly across all seasons ($\prod_{\text{season}=i} p_i = 0.0091$) it becomes apparent that within the larger, expected warming trend of 1980–present, Greenland experienced an unexpected cooling hiatus during the 2003–2017 GRACE record (see Figure 3 & Table 2). It is important to note that, regardless of fitted trends, the majority of the 10 warmest seasons of the 1980–2017 record have occurred during the GRACE record (6/10 Winters, 8/10 Springs, 8/10 Summers, 6/10 Falls), and for the first decade of GRACE data, all but one Summer season on the Greenland Ice Sheet had mean temperatures above the 1980–2017 average see (Figure 3 & Table 3).

In addition to differences in near surface temperature anomaly trends found in different seasons and decades, there is also significant spatial heterogeneity temperature anomaly trends across the Greenland Ice Sheet. I calculated a linear fit for temperature anomaly at each node of the grid across Greenland (see Figure **??**) for years between 1980–2017, from the beginning of GRACE until the end of 2012 (2003–2012), and for the entire GRACE record (2003–2017), illustrated in Figure 4. Those trends within those three time periods have very different features, characterized by widespread warming in all seasons (1980–2017), general cooling in non-summer seasons with strong Summer warming in the SW region (2003–2012), and general cooling across the vast majority of the ice sheet in all seasons (2003–2017) (Figure 4).

	Summer (JJA)		Winter (DJF)	
	Year	**T2M anom. °C**	**Year**	**T2M anom. °C**
1	2012 (1)	2.19 ± 0.51	2010	5.28 ± 0.70
2	2007 (7)	1.59 ± 0.56	1980	3.23 ± 2.19
3	2010 (3)	1.32 ± 0.77	2011	3.06 ± 2.67
4	2003 (8)	1.07 ± 1.02	2003	2.75 ± 1.59
5	2004 (13)	0.95 ± 0.55	2007	2.34 ± 1.84
6	2016 (2)	0.86 ± 0.50	2013	2.25 ± 0.34
7	2008 (9)	0.73 ± 0.25	1986	1.75 ± 2.92
8	1998	0.63 ± 0.59	2009	1.70 ± 0.48
9	2005 (5)	0.62 ± 1.22	1996	1.46 ± 0.48
10	2002	0.56 ± 1.60	1987	2.35 ± 3.79

Table 3: Top 5 years ranked by highest mean 2m air temperature for Summer and Winter seasons over the Greenland Ice Sheet (1980–2017). Adjacent to the year, in parentheses, is that year's rank by greatest mass loss (2003–2017). Mean temperature is the mean of the three monthly means in that season, and the reported error is the standard of deviation of the three monthly means in that season. Despite a downward drift in mean temperature between 2003–2017, a majority of the top ten warmest seasons on record occurred within that time frame. Note the separation of 2012 from the next closest years, making it the warmest summer on record. Worth noting is that 2013, the year of least mass loss on the GRACE record, ranks as the 5th coldest Summer season in the 1980–2017 record, and the coldest Summer season of the GRACE time period.

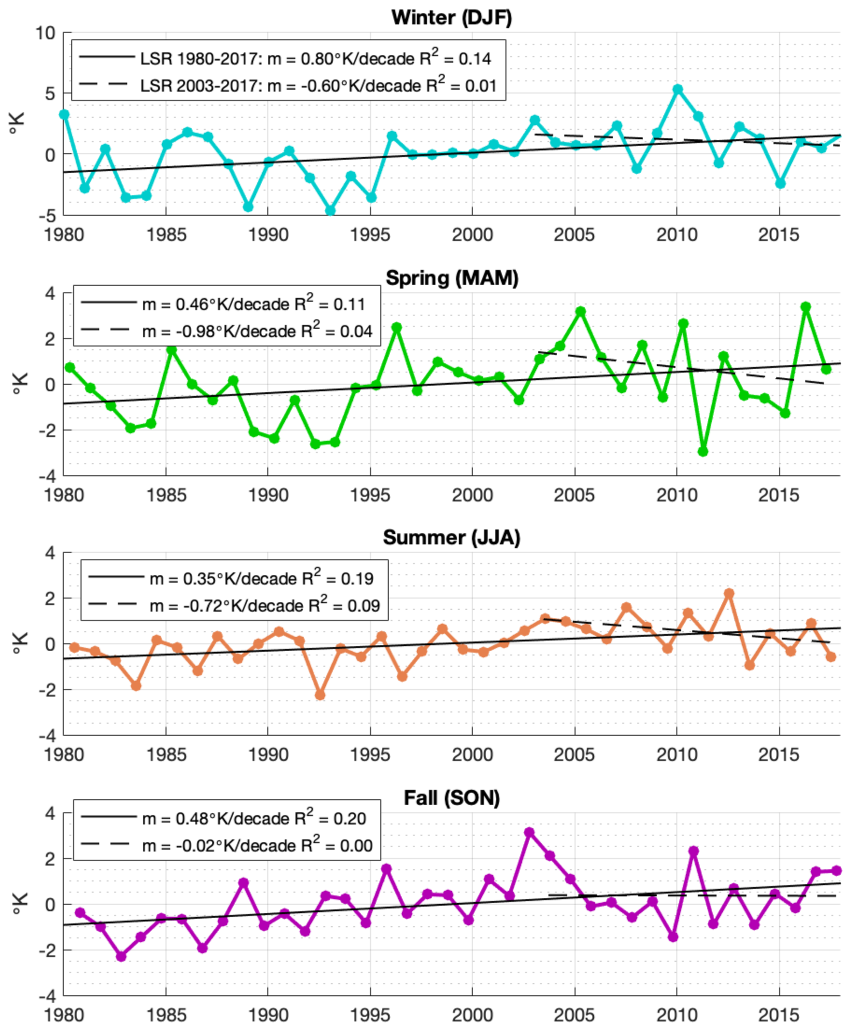

Figure 3: Seasonal trends in MERRA-2 2m air temperature across the Greenland Ice Sheet for 1980–2017. Plotted points are the seasonal mean for each year, and are fit with a type-1 least squares regression for the full time period (solid) and the GRACE time period (dashes). Note that between 1980–2017 Winter temperatures warmed more than summer temperatures, while during the GRACE time period (2003–2017) Summer temperatures dropped more than Winter temperatures. Table 2 contains an analysis of the significance of each trend and its confidence interval, showing that the seasonal trends in mean monthly temperature over the full time period are significant, while the seasonal trends over the GRACE period are not significantly differentiable (in both *p*-value and confidence interval) from trends in random data drawn randomly from a similar normal distribution.

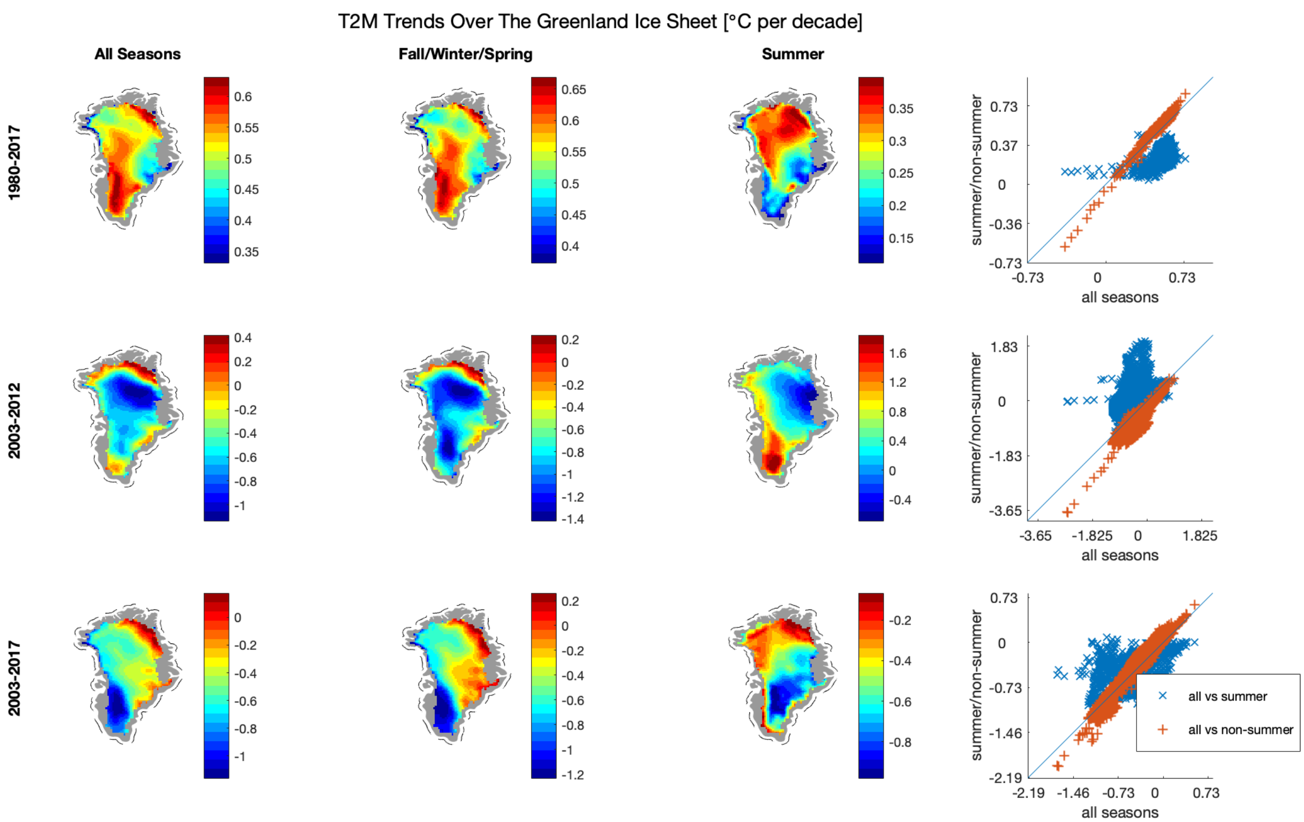
T2M Trends Over The Greenland Ice Sheet [°C per decade]
All Seasons
Fall/Winter/Spring
Summer
1980-2017
2003-2012
2003-2017
summer/non-summer
all seasons
all vs summer
all vs non-summer

Figure 4

Appendix A: Data and code sources

RL05 spherical harmonic coefficients for the time-variant geopotential field from the Center for Space Research data processing center at The University of Texas at Austin are available at:

`ftp://podaac.jpl.nasa.gov/allData/grace/L2/CSR/RL05`

Coefficients describing Earth's center of mass (spherical harmonic degree 1, from Swenson et al., 2008) are available at:

`ftp://podaac-ftp.jpl.nasa.gov/GeodeticsGravity/tellus/L2/degree_1/`

Coefficients describing Earth's oblateness (spherical harmonic degree 2, order 0, from Cheng et al., 2013) are available at:

`ftp://ftp.csr.utexas.edu/pub/slr/degree_2/`

Index values for the North Atlantic Oscillation are calculated by the National Weather Service Climate Prediction Center (see CPC, 2012), with normalized monthly average values since January 1950 available at:

`ftp://ftp.cpc.ncep.noaa.gov/wd52dg/data/indices/nao_index.tim`

Normalized daily values since January 1950 are available at:

`ftp://ftp.cpc.ncep.noaa.gov/cwlinks/norm.daily.nao.index.b500101.current.ascii`

MERRA-2 atmospheric reanalysis data are calculated by the NASA Global Modeling and Assimilation Office (GMAO) as part of the activities of NASA's Science Mission Directorate, and are archived and distributed by the Goddard Earth Sciences Data and Information Services Center (GES-DISC). All data was accessed between September 2018 and April 2019.

A graphical user interface for generating data download links for specific subsets of variables, space, and time is available at: `https://disc.gsfc.nasa.gov`

Data used in this study can be directly accessed at the following addresses:

https://goldsmr4.gesdisc.eosdis.nasa.gov/data/MERRA2_MONTHLY/M2SMNXSLV.5.12.4/

https://goldsmr4.gesdisc.eosdis.nasa.gov/data/MERRA2/M2T1NXSLV.5.12.4/

https://goldsmr4.gesdisc.eosdis.nasa.gov/data/MERRA2/M2T1NXRAD.5.12.4/

Northern Hemisphere Land-Ocean Temperature Index anomalies from NASA's Goddard Institute for Space Studies Surface Temperature Analysis (GISTEMP v3, see Hansen et al., 2010) were accessed in March 2019 and are available at:

https://data.giss.nasa.gov/gistemp/tabledata_v3/NH.Ts+dSST.csv

MATLAB code for the expansion and manipulation of spherical harmonic eigenfunctions into Slepian bases and manipulation of GRACE files is borrowed and adapted from:

https://github.com/csdms-contrib/

MATLAB code developed for this project, including functions for executing the wavelet analysis and scripts for generating figures, can be accessed at:

https://github.com/bgetraer/slepian_bgetraer/

References

Bevis, M., Harig, C., Khan, S. A., Brown, A., Simons, F. J., Willis, M., Fettweis, X., van den Broeke, M. R., Madsen, F. B., Kendrick, E., Caccamise, D. J., van Dam, T., Knudsen, P., & Nylen, T., 2019. Accelerating changes in ice mass within Greenland, and the ice sheet's sensitivity to atmospheric forcing, *Proceedings of the National Academy of Sciences*, **116**(6), 1934–1939, doi: 10.1073/pnas.1806562116.

Bosilovich, M. G., Lucchesi, R., & Suarez, M., 2016. MERRA-2: File Specification, *GMAO Office*, **Note No. 9 (Version 1.1), available from `http://gmao.gsfc.nasa.gov/pubs/office_notes`**.

Cheng, M., Tapley, B. D., & Ries, J. C., 2013. Deceleration in the Earth's oblateness, *Journal of Geophysical Research: Solid Earth*, **118**(2), 740–747, doi: 10.1002/jgrb.50058.

CPC, 2012. Northern Hemisphere Teleconnection Patterns, *National Weather Service Climate Prediction Center (Eds)*, **published online, last modified January 2012 at `https://www.cpc.ncep.noaa.gov/data/teledoc/telecontents.shtml`**.

Enderlin, E. M., Howat, I. M., Jeong, S., Noh, M.-J., van Angelen, J. H., & van den Broeke, M. R., 2014. An improved mass budget for the Greenland ice sheet, *Geophysical Research Letters*, **41**(3), 866–872 doi 10.1002/2013GL059010.

Gelaro, R., McCarty, W., SuÃ¡rez, M. J., Todling, R., Molod, A., Takacs, L., Randles, C. A., Darmenov, A., Bosilovich, M. G., Reichle, R., Wargan, K., Coy, L., Cullather, R., Draper, C., Akella, S., Buchard, V., Conaty, A., da Silva, A. M., Gu, W., Kim, G.-K., Koster, R., Lucchesi, R., Merkova, D., Nielsen, J. E., Partyka, G., Pawson, S., Putman, W., Rienecker, M., Schubert, S. D., Sienkiewicz, M., & Zhao, B., 2017. The Modern-Era Retrospective Analysis for Research and Applications, Version 2 (MERRA-2), *Journal of Climate*, **30**(14), 5419–5454, doi: 10.1175/JCLI–D–16–0758.1.

Getraer, B., 2017. Resolving and Contextualizing the Signal of Greenland Ice Loss 2014–2017, *Princeton Department of Geosciences*, **Fall Junior Paper, unpublished**.

Getraer, B., 2018. Regional Forcing of Greenland Ice Loss 2002–2017, *Princeton Department of Geosciences*, **Spring Junior Paper, unpublished**.

Hahn, L., Ummenhofer, C. C., & Kwon, Y.-O., 2018. North Atlantic Natural Variability Modulates Emergence of Widespread Greenland Melt in a Warming Climate, *Geophysical Research Letters*, **45**(17), 9171–9178.

Hanna, E., Fettweis, X., Mernild, S. H., Cappelen, J., Ribergaard, M. H., Shuman, C. A., Steffen, K., Wood, L., & Mote, T. L., 2013. Atmospheric and oceanic climate forcing of the exceptional Greenland ice sheet surface melt in summer 2012, *International Journal of Climatology*, **34**(4), 1022–1037.

Hansen, J., Ruedy, R., Sato, M., & Lo, K., 2010. Global Surface Temperature Change, *Reviews of Geophysics*, **48, RG4004**, 1–29, doi:10.1029/2010RG000345.

Harig, C. & Simons, F. J., 2015. Accelerated West Antarctic ice mass loss continues to outpace East Antarctic gains, *Earth Planet. Sci. Lett.*, **415**, 134–141, doi: 10.1016/j.epsl.2015.01.029.

Harig, C. & Simons, F. J., 2016. Ice mass loss in Greenland, the Gulf of Alaska, and the Canadian Archipelago: Seasonal cycles and decadal trends, *Geophysical Research Letters*, **43**(7), 3150–3159, doi: 10.1002/2016GL067759.

Hartmann, D., Tank, A. K., Rusticucci, M., Alexander, L., Brönnimann, S., Charabi, Y., Dentener, F., Dlugokencky, E., Easterling, D., Kaplan, A., Soden, B., Thorne, P., Wild, M., & Zhai, P., 2013. *Climate Change 2013: The Physical Science Basis. Contribution of Working Group I Contribution to the Fifth Assessment Report of the Intergovernmental Panel on Climate Change*, chap. Observations: Atmosphere and Surface, p. doi: 10.1017/CBO9781107415324, Cambridge Univ. Press.

Hearty, T. J., Lee, J. N., Wu, D. L., Cullather, R., Blaisdell, J. M., Susskind, J., & Nowicki, S. M. J., 2018. Intercomparison of Surface Temperatures from AIRS, MERRA, and MERRA-2 with NOAA and GC-Net Weather Stations at Summit, Greenland, *Journal of Applied Meteorology and Climatology*, **57**(5), 1231–1245.

Khan, S. A., Aschwanden, A., Bjørk, A. A., Wahr, J., Kjeldsen, K. K., & Kjær, K. H., 2015. Greenland ice sheet mass balance: a review, *Reports on Progress in Physics*, **78**(4), 046801.

Kosaka, Y. & Xie, S.-P., 2013. Recent global-warming hiatus tied to equatorial Pacific surface cooling, *Nature*, **501**(7467), 403.

Mattingly, K., Mote, T., & Fettweis, X., 2018. Atmospheric River Impacts on Greenland Ice Sheet Surface Mass Balance, *Journal of Geophysical Research: Atmospheres*, **123**, 8538–8560, doi: 10.1029/2018JD028714.

McMillan, M., Leeson, A., Shepherd, A., Briggs, K., Armitage, T. W., Hogg, A., Munneke, P. K., van den Broeke, M., Noël, B., van de Berg, W. J., Ligtenberg, S., Horwath, M., Groh, A., Muir, A., & Gilbert, L., 2016. A high-resolution record of Greenland mass balance, *Geophysical Research Letters*, **43**(13), 7002–7010, doi: 10.1002/2016GL069666.

NCAR, 2019. The Climate Data Guide: Hurrell North Atlantic Oscillation (NAO) Index (PC-based), *National Center for Atmospheric Research Staff (Eds)*, **published online, last modified January 2019 at `https://climatedataguide.ucar.edu/climate-data/hurrell-north-atlantic-oscillation-nao-index-pc-based`**.

Nerem, R. S., Beckley, B. D., Fasullo, J. T., Hamlington, B. D., Masters, D., & Mitchum, G. T., 2018. Climate-change–driven accelerated sea-level rise detected in the altimeter era, *Proceedings of the National Academy of Sciences*, **115**(9), 2022–2025, doi: 10.1073/pnas.1717312115.

NOAA, 2019. State of the Climate: Global Climate Report for Annual 2018, *National Centers for Environmental Information*, **published online, January 2019 at `https://www.ncdc.noaa.gov/sotc/global/201813`**.

Pattyn, F., Ritz, C., Hanna, E., Asay-Davis, X., DeConto, R., Durand, G., Favier, L., Fettweis, X., Goelzer, H., Golledge, N. R., et al., 2018. The Greenland and Antarctic Ice Sheets Under 1.5Â° C Global Warming, *Nature Climate Change*, p. 1.

Reeves Eyre, J. & Zeng, X., 2017. Evaluation of Greenland near surface air temperature datasets, *The Cryosphere*, **11**(4), 1591–1605.

Rückamp, M., Greve, R., & Humbert, A., 2018. Comparative Simulations of the Evolution of the Greenland Ice Sheet Under Simplified Paris Agreement Scenarios with the Models SICOPOLIS and ISSM, *Polar Science*.

Solomon, A., Shupe, M. D., & Miller, N. B., 2017. Cloud-Atmospheric Boundary Layer-Surface Interactions on the Greenland Ice Sheet during the July 2012 Extreme Melt Event, *Journal of Climate*, **30**(9), 3237–3252.

Swenson, S., Chambers, D., & Wahr, J., 2008. Estimating geocenter variations from a combination of GRACE and ocean model output, *Journal of Geophysical Research: Solid Earth*, **113**(B8), doi: 10.1029/2007JB005338.

Van Angelen, J., Van den Broeke, M., Wouters, B., & Lenaerts, J., 2014. Contemporary (1960–2012) evolution of the climate and surface mass balance of the Greenland ice sheet, *Surveys in Geophysics*, **35**(5), 1155–1174.

Vaughan, D., Comiso, J., Allison, I., Carrasco, J., Kaser, G., Kwok, R., Mote, P., Murray, T., Paul, F., Ren, J., Rignot, E., Solomina, O., Steffen, K., & Zhang, T., 2013. *Climate Change 2013: The Physical Science Basis. Contribution of Working Group I Contribution to the Fifth Assessment Report*, chap. Observations: Cryosphere, p. doi: 10.1017/CBO9781107415324, Cambridge Univ. Press.

Velicogna, I., 2009. Increasing rates of ice mass loss from the Greenland and Antarctic ice sheets revealed by GRACE, *Geophysical Research Letters*, **36**(19), doi 10.1029/2009GL040222, L19503.

Westergaard-Nielsen, A., Karami, M., Hansen, B. U., Westermann, S., & Elberling, B., 2018. Contrasting temperature trends across the ice-free part of Greenland, *Scientific reports*, **8**(1), 1586.

Zwally, H. J., Giovinetto, M. B., Beckley, M. A., & Saba, J. L., 2012. Antarctic and Greenland Drainage Systems, GSFC Cryospheric Sciences Laboratory, *Available at http://icesat4.gsfc.nasa.gov/cryo_data/ant_grn_drainage_systems.php. Accessed October 2018*, **1**, 2015.